P8.8   **MID-SUMMER GAP WINDS AND LOW-LEVEL CIRCULATION OVER THE EASTERN TROPICAL PACIFIC**

Rosario Romero-Centeno*, Jorge Zavala-Hidalgo, and G. B. Raga
Centro de Ciencias de la Atmosfera, Universidad Nacional Autonoma de Mexico, Mexico City, Mexico

1. INTRODUCTION

The northeastern tropical Pacific (NETP), between 0° and 25°N and east of 120°W, is characterized by outstanding oceanic and atmospheric conditions leading to important air-sea interaction processes in a wide range of spatial and temporal scales. Among them worth of mention are the equatorial cold tongue, the eastern Pacific warm pool and the Intertropical Convergence Zone (ITCZ). Each one of these features has received special attention and research in a wide number of publications (e.g. Amador et al. 2005, and references within).

Besides the above features of the NETP, the special orography of the continents on its eastern boundary, combined with the meteorological conditions, produces strong winds through the low-elevation gaps of the Sierra Madre del Sur in southern Mexico and the Central American cordillera (Fig. 1). The three major mountain gaps are located at the Isthmus of Tehuantepec, the lake district of Nicaragua and Panama, and the strong offshore winds in the lee of these mountain gaps are known as the Tehuantepec, Papagayo and Panama jets, respectively. The influence of these wind jets on local processes over the adjacent Pacific waters, such as the generation of large warm oceanic eddies, intense offshore currents, increase in turbulent heat fluxes, considerable drop of the SST by upwelling and entrainment of subsurface water, and increase in biological activity, has motivated many studies, which have especially focused over the Gulf of Tehuantepec.

The generation mechanism of the Tehuantepec jet during boreal winter, when it is strongest and more frequent, has been widely documented: large sea level pressure differences between the Gulf of Mexico and the

eastern Pacific, caused by the southeastward migration of high pressure systems associated with cold-air outbreaks originating over North America, generate air flows that are blocked by the cordillera and then channeled through the mountain gap (e.g. Roden 1961; Parmenter 1970; Clarke 1988; Lavín et al. 1992; Schultz et al. 1997; Steenburgh et al. 1998). Frequently, as the high pressure system penetrates far to the south, the Tehuantepec jet is followed a few days later by the Papagayo and Panama jets. However, sometimes the Papagayo and Panama jets are influenced by trade wind fluctuations and tropical circulations that have little or no effect on the Tehuantepec jet (Chelton et al. 2000a). Also, there are differences among the three jets in intensity, orientation, time scales, and seasonality which result in different oceanic and atmospheric responses (Chelton et al. 2000a,b; Kessler 2002; Xie et al. 2005).
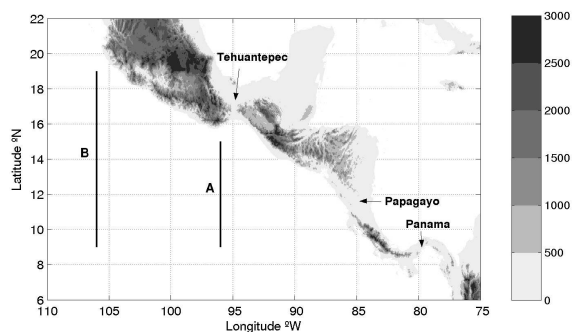

Figure 1. Location of the major low-elevation mountain gaps in southern Mexico and Central American cordillera. Gray shading represents elevation in meters according to the color bar. Thick lines labeled A and B show the location of the sections across which mass transports are calculated (see sec. 3.1).

At seasonal scale, the intensity of the three jets weakens in spring and summer, but there is a slight strengthening of the Tehuantepec and Papagayo jets during July-August whose origin, at least in the case of the Tehuantepec jet, has been attributed to a sea level pressure difference between the western Atlantic and the

---

* *Corresponding author address:* Rosario Romero-Centeno, Centro de Ciencias de la Atmosfera, UNAM, Mexico City, Mexico; e-mail: romero@atmosfera.unam.mx.

eastern Pacific caused by the mid-summer westward extension and intensification of the Azores-Bermuda high (Romero-Centeno et al. 2003). This strengthening of the jets is in phase with the mid-summer drought in southern Mexico and Central America, a climatological phenomenon unique to the western hemisphere, where rainfall amounts reduce by roughly 40% in late July and early August compared to June and September (Magaña et al. 1999; Curtis 2004). Magaña et al. (1999) proposed that the local air-sea interactions in the NETP lead to changes in the convection pattern. SST seasonal fluctuation along with fluctuations in the low-level convergent flow and an intensification of the trade winds, which they suggest is part of the dynamical response to the intensity of the convective forcing of the ITCZ, produce the bimodal distribution of precipitation during the summer season. Recently, Magaña and Caetano (2005) proposed a combined effect of SST changes and subsidence related to direct circulations as a better explanation of the convective activity observed during summer over the NETP. At present, however, the influence and possible link between the mid-summer intensification of the Tehuantepec and Papagayo wind jets and the atmospheric circulation and convection pattern over the NETP still remains to be completely understood.

This work discusses the mid-summer strengthening of the Tehuantepec and Papagayo jets and its impact on the low-level circulation of the NETP, the possible causes and implications. The near-surface wind analysis is performed by using the increasingly utilized National Aeronautics and Space Administration's QuikSCAT/SeaWinds scatterometer (QSCAT) winds. Recent studies have demonstrated that, currently, the QSCAT wind product is the best to resolve the wind jets in different space-time scales and is an excellent tool to characterize the dynamical state of the lower troposphere with a high degree of accuracy (Chelton et al. 2004; Bordoni et al. 2004). The vertical structure of the wind and pressure fields is analyzed using data from the European Centre for Medium-Range Weather Forecasts 40-Years Reanalysis (ERA-40).

2. DATA

Previous studies have shown that scatterometers are unique among satellite remote sensors in their ability to measure wind speed and direction over the global surface waters. In particular, QSCAT provide wind measurements with a much greater spatial and temporal coverage than in situ observations or any previous scatterometer missions, and significantly higher resolution than what currently provided by numerical weather prediction models or reanalysis wind products (Bourassa et al. 2003; Chelton et al. 2004). QSCAT collects data within a 1,800-km wide swath covering roughly 93% of the oceanic surface in one day, with a 25-km spatial resolution, and measures wind speed with an accuracy of ± 2 m s^{-1} and wind direction with an accuracy of $\pm 20°$ or better (http://winds.jpl.nasa.gov/missions/quikscat). In the present study, daily near-surface vector winds are processed and analyzed for the period August 1999 - December 2004 over the region 0-33ºN, 130ºW-75ºW.

QSCAT winds were downloaded from the Center for Ocean-Atmospheric Prediction Studies webpage (http://coaps.fsu.edu/cgi-bin/ qscat/wind-swath-ku2001), consisting of the Remote Sensing Systems Ku-2001 swath data sets. Winds are referenced to a height of 10 m and the data files include wind speed, wind direction, time, latitude, and longitude. Zonal (u) and meridional (v) wind components are calculated from the wind speed and direction information, excluding data flagged as rain contaminated. u and v are averaged within 0.5º x 0.5º lat-lon boxes, taking into account the time of measurement, and then daily and monthly mean winds and divergence fields are calculated. Divergence is calculated using a centered difference scheme. Long-term monthly means for the analyzed period are then estimated from the monthly averages.

The European Centre for Medium-Range Weather Forecasts data from the ERA-40 reanalysis project (http://data.ecmwf.int/data/ d/era40_daily), which used in-situ and remotely-sensed by satellite observations and data assimilation techniques applied at T159 (~140 km) resolution along with a refined numerical model, are used to get a three-dimensional depiction of the atmosphere over the study region. ERA-40, 4 times daily, wind components and geopotential height data at different pressure levels on a 2.5° grid are used to derive the corresponding long-term monthly means for the period 1960-2001. ERA-40 monthly mean

sea level pressures for the same period are also used.

3. RESULTS

3.1 Gap winds seasonal variability

Long-term monthly mean wind vectors from the QuikSCAT scatterometer for the period August 1999 - December 2004 show a strong seasonal signal in the NETP, the Gulf of Mexico, and the Caribbean regions (Fig. 2). One of the more outstanding features is the signal associated with the winds crossing through the low-elevation mountain gaps of the cordillera in southern Mexico and Central America (see Fig. 1 for location), which has been documented in previous works. The signal of the intense winds over the Gulf of Tehuantepec (*Tehuanos*) is noticeable from October, and the winds over the Gulf of Papagayo (*Papagayos*) are weakly distinguishable since November (Figs. 2j-k). During boreal winter (Dec-Feb) these gap winds are very evident, with the *Tehuanos* showing a prevalent meridional orientation and the *Papagayos* a more pronounced zonal orientation (Figs. 2a-b, 2l). During this season, the *Tehuanos* extend far to the south, merging with the *Papagayos* and the Pacific northeast trades and turning westward. The *Tehuanos* and *Papagayos* weaken in March (Fig. 2c) and they are barely visible in April (Fig. 2d). In January and February also the winds crossing through Panama are present in the monthly averages, being roughly north-south oriented as the *Tehuanos*, and they are still distinguishable during March and even April (Figs. 2a-d). In general, winds are very weak during spring-summer in the whole NETP warm pool area, except for a slight intensification of the Tehuantepec and Papagayo jets during July and August, being less intense in the latter (Fig. 2g-h).

During winter and spring months (from December through April), when the northerly trades are more intense, winds in the NETP are mainly easterlies blowing from the coast to the western Pacific (Fig. 2a-d, 2l). In May, this pattern begins to change: southerly trades start intensifying, while light westward winds north of 7°N cover the convergence zone and the warm pool area (Fig. 2e). In June, while the northerly trades are relatively weak, the southerly trades keep intensifying and slightly reverse over the NETP around 10°N, heading east from ~117°W (Fig. 2f). This circulation pattern favors moisture transport into the continent, coinciding with the first maximum of the bimodal distribution in precipitation over central-southern Mexico and Central America (Magaña et al. 1999).

However, in July and, though less intense, in August, when a slight strengthening of the Tehuantepec and Papagayo wind jets is observed, the low-level flow into the region of light winds shows again a westward orientation (Figs. 2g-h). This westward flow is not restricted to the area near the coast, but is observed several hundred kilometers (~2,200 km) offshore over the NETP. This circulation pattern seems to block the northward penetration of the southeast trades, despite their strength and eastward orientation, and inhibits the low-level moisture transport into the continent, which coincides with the mid-summer drought observed in the region during late July-early August.

The wind pattern changes abruptly in September (Fig. 2i), featuring imperceptible wind jets, the weakest northerly trades, the northernmost penetration of the southerly trades and a low-level westerly flow over the NETP that favors the moisture transport into the continent. During this month, the precipitation increases again in the region, when the second maximum of its bimodal distribution is observed. Around October, this wind circulation pattern begins weakening, giving rise to that observed during winter and spring.

Monthly mean mass transports associated with the low-level easterly flow over the NETP through the two sections 9°N-15°N at 96°W and 9°N-19°N at 106°W (see Fig. 1 for its location), assuming a 1m-thick near-surface atmospheric layer and a constant air density of 1.225 kg m^{-3}, show similar westward transports just west of the Gulf of Tehuantepec and ten degrees far to the west (Fig. 3). The seasonal variations at both sections show larger westward transports during winter and smaller toward the summer, with a relative maximum in July-August. From November to April the westward transports are slightly smaller at 96°W; in May-August they are slightly smaller at 106°W, which reaches zero in June for this section.
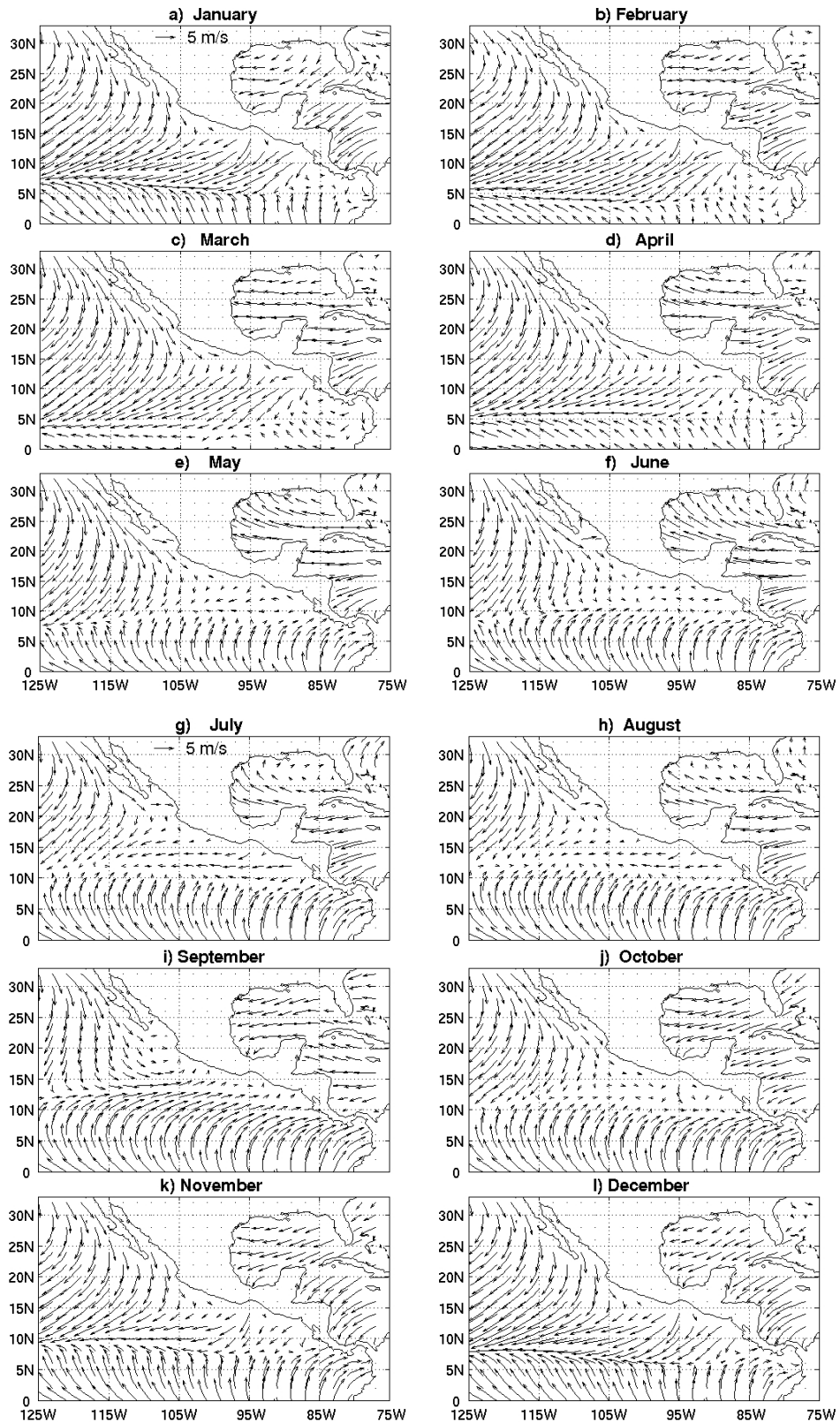
Figure 2. Long-term monthly mean vector winds from QSCAT scatterometer for the period Aug 1999-Dec 2004.

6

In September, the westward mass transport is zero at both sections, and is also zero in October at 106°W while it is relatively small at 96°W. This behavior tracks with the seasonal intensity variation of the Tehuantepec and Papagayo jets, suggesting that the low-level easterly flow during July-August over the NETP is induced by the intensification of these two wind jets.
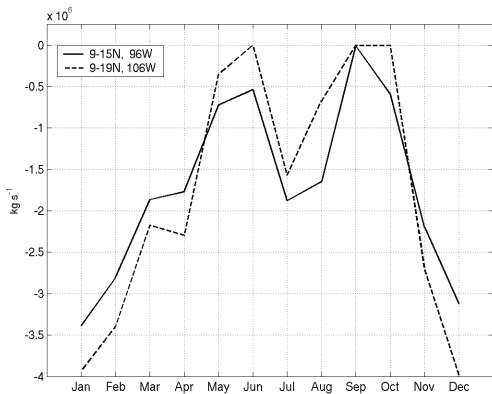

Figure 3. Long-term monthly mean westward mass transports through the sections A (9°N-15°N, 96°W) and B (9°N-19°N, 106°W) shown in figure 1 from QSCAT data.

3.2 Wind divergence field

The long-term monthly mean wind divergence fields derived from the QSCAT vector winds are an important tool to analyze the impact of the gap winds over the eastern Pacific ITCZ (Fig. 4). These fields clearly show the seasonal fluctuations of the ITCZ, which shifts to the south during boreal winter months and to the north in summer. The extent of the displacement appears more pronounced in the western region of the NETP. In November, December and January, when the northerly and southerly trades are both relatively intense, a narrow band of strong convergence is observed centered at around 7°N (Figs. 4a, 4k-l). In February, the southerly trades begin weakening and the convergence is less intense (Fig. 4b). March is the month with the maximum southward displacement of the ITCZ: the northerly trades are very strong, the southerly trades are relatively weak and the convergence is small (Fig. 4c). The northward migration of the ITCZ begins in April, when the southerly trades begin strengthening (Fig. 4d).

The divergence fields also clearly show the divergent winds associated with the Tehuantepec, Papagayo, and Panama jets, as well as small convergence areas at both sides of the jets (Fig. 4a-d). During the winter months, when the jets are the strongest, the influence of their associated divergent winds over the configuration of the ITCZ is very noticeable, suggesting that the jets affect the location and shape of the ITCZ in the easternmost NETP, pushing it southward and keeping it confined away from the coast.

From May onwards, the southerly trades gradually intensify and the convergence strengthens and covers a wider meridional extent than what observed in winter (Fig. 4e). In June the divergence field is similar to that in May, with some scattered convergence areas closer to the continent, east of ~107°W (Fig. 4f). It is important to remind here that light low-level westerlies are observed in June over the NETP, as described in the previous section. During July-August, however, the low-level circulation over the NETP reverses and the intensified wind jets and easterlies seem to displace the convergence areas to the west of ~107°W, away from the coast, while keeping the ITCZ confined to the south of the jets (Fig. 4g-h). This pattern is similar to that observed in winter, although less intense. The change in the circulation pattern in September causes convergence areas to cover most of the NETP northeastern basin and favors the moisture transport to southern Mexico and Central America (Fig. 4i). These results are consistent with the bimodal distribution in precipitation observed during summer in southern Mexico and Central America.

3.3 Sea level pressure variations

Long-term monthly mean sea level pressures (SLP) in the region 0-50°N, 150°W-10°W from ERA-40 reanalysis data, show the two permanent subtropical high-pressure systems around 30?N over the northeastern Pacific and the subtropical Atlantic (known as the Azores-Bermuda high, ABH), both showing a clear seasonal variability in location and strength (Fig. 5). Also evident are a third non-permanent system over the continental U.S. and a belt of low pressures dominating the tropical areas. These pressure systems determine, to a large extent, the monthly course of the low-level wind circulation over the region.
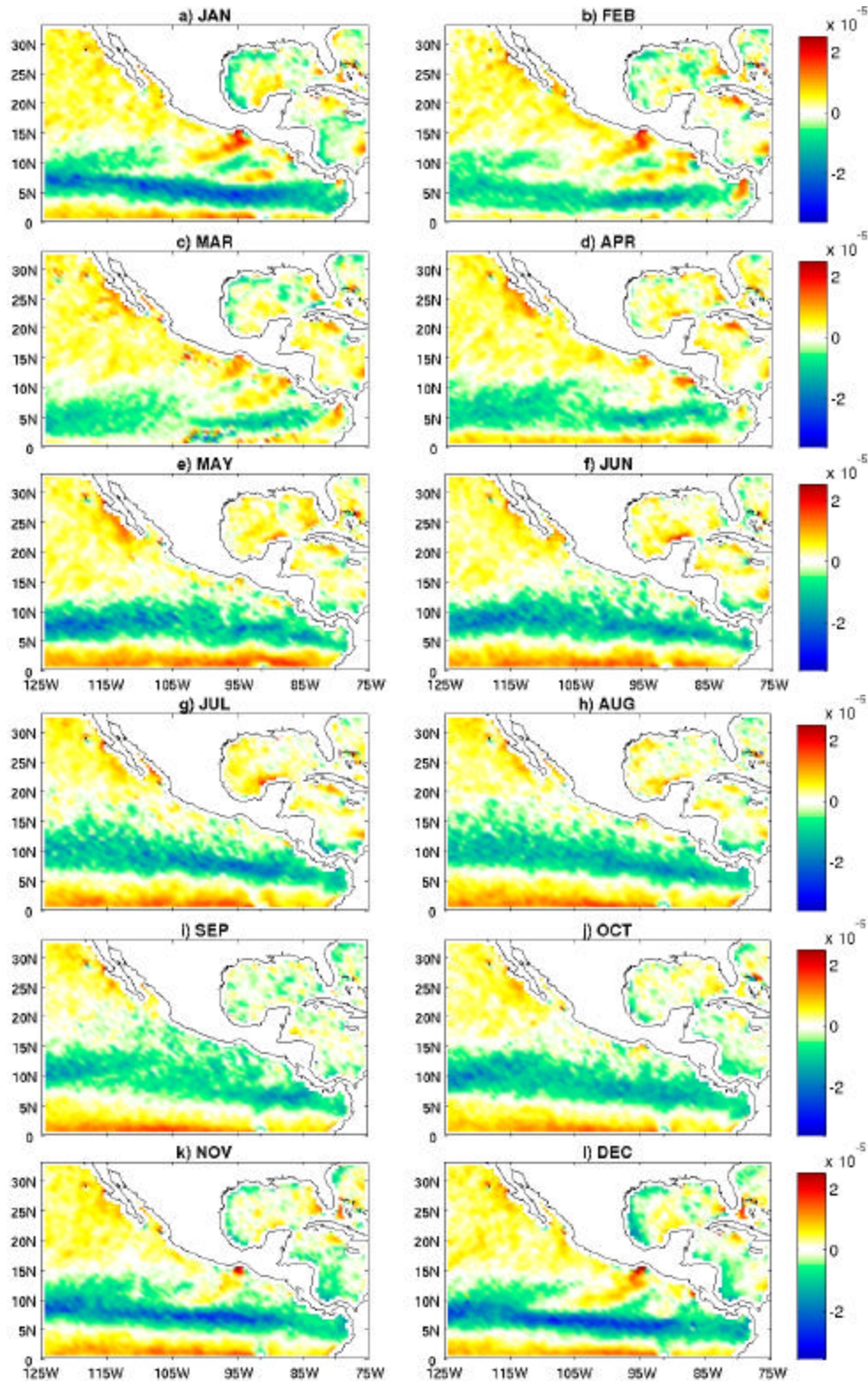
5

Figure 4. Long-term monthly mean wind divergence from QSCAT data.

A feature of the ABH seasonality is its bimodal behavior in intensity (Fig. 5), with an absolute maximum during July, a relative maximum in January, and minima during October-November and April. The absolute maximum of the ABH intensity in July coincides with the maximum westward displacement of its center over the subtropical Atlantic, while in January the center of the ABH is at its farthest eastern position. The atmospheric SLP anomalies from the June-September mean, show a large area of positive values in July that extends from the central subtropical Atlantic, where the anomaly is larger, to the Mexican Pacific coasts, where it is smaller (Fig. 6). The SLP anomaly map for September contrasts with that for July, showing areas of relatively large negative anomalies that cover most of the subtropical Atlantic and the northeastern Pacific. These two areas of negative SLP anomalies are separated by a positive anomaly area over North America and Mexico.

Figures 5 and 6 indicate that the maximum westward extension and intensification of the ABH during mid-summer establishes an across-gap pressure difference at the Isthmus of Tehuantepec (~4 hPa in July), larger than that observed during the rest of the summer months, that induces the strengthening of the Tehuantepec jet. Figures 5 and 6 show, however, that there is no such across-gap pressure difference that might induce the intensification of the Papagayo jet during this time of the year. This is because the winds through the Isthmus of Tehuantepec flow in the same direction as the pressure gradient (perpendicular to the isobars) owing to the north-south orientation of the mountain gap, while the east-west orientation of the Papagayo gap favors the funneling of the western Caribbean zonal winds flowing roughly parallel to the ABH isobars. Therefore, the mid-summer maximum westward extension and intensification of the ABH cause the strengthening of both the Tehuantepec and Papagayo jets, albeit by means of a different dynamical process. These results agree with Chelton et al. (2000a) who, based on the 9-month NSCAT mission observations, concluded that the mechanism that controls the Papagayo and Panama jets is very different from the across-gap pressure gradients that control the Tehuantepec jet during winter.

Consequently, the main physical mechanism that produces the Tehuantepec jet intensification during July-August is the same as that during winter, a large across-gap pressure gradient, but the large-scale systems involved are different in each season.
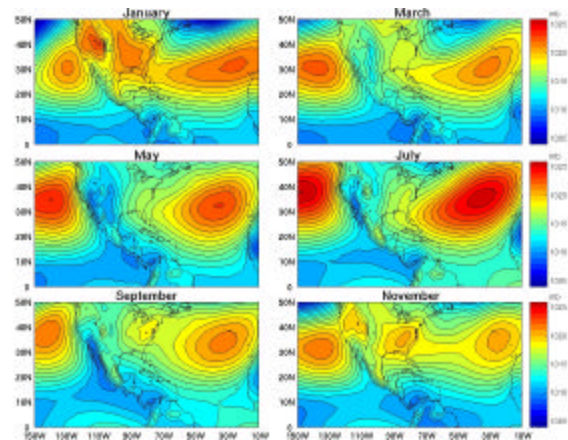

Figure 5. Long-term monthly mean sea level pressures from ERA-40 data for 1960-2001.
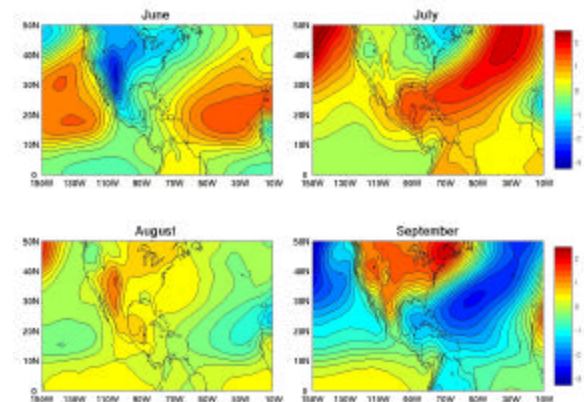

Figure 6 Mean sea level pressure anomalies from the Jun-Sep mean for the June, July, August and September climatologies from ERA-40 data.

3.4 Upper level pressure and wind variations

The westward displacement and strengthening of the ABH center is observed not only at the surface but also at upper levels. The long-term monthly averages of geopotential height from June through September for the 925 and 700-mb surfaces over the region 0-35°N and 130-70°W (Fig. 7, bottom and next to bottom panels, respectively), show these ABH

features during July-August, with larger pressure gradients between the far-eastern NETP and the southern Gulf of Mexico-western Caribbean Sea than those observed in June and September.

At the lower levels (approximately up to 850-mb, not shown), the distribution and location of the Atlantic and Pacific highs, separated by low pressures over the continent, establish relatively strong zonal pressure gradients north of ~18⁰N and relatively strong meridional pressure gradients between ~12°N and 18°N. These pressure patterns determine complex wind fields that are also affected by the orography. In the 700 and 500-mb geopotential height maps (Fig. 7, middle panels), the Pacific high is not clearly distinguished in mid-summer since the subtropical Atlantic high extends more westward than at lower levels, producing intense easterlies over the north NETP, the Gulf of Mexico and the Caribbean.
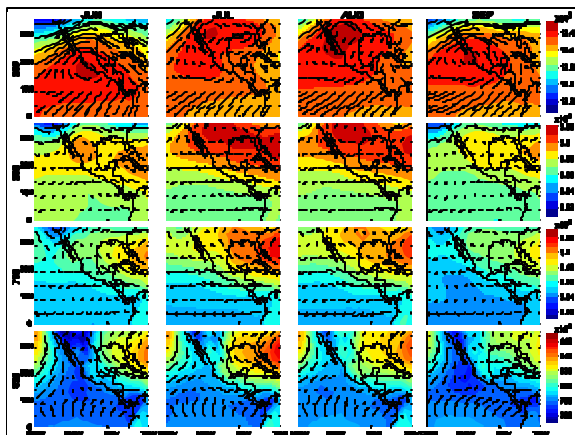

Figure 7. Long-term monthly mean geopotential height and winds for the 925, 700, 500, and 200-mb surfaces from ERA-40 data.

The geopotential height long-term monthly maps for the 200-mb surface (Fig. 7, top panels) also show patterns that change within the summer, causing the wind fields to vary from month to month over the displayed area. During the four summer months, intense divergent northeasterly winds south of ~10°N are evident, probably associated with the ITCZ at lower levels. In June, westerly winds are observed north of ~17°N on the northern flank of the anticyclonic circulation associated with the high pressure system centered at ~18°N, 103°W. The center of this high pressure is displaced

northwestward during July-August, which implies a migration of the convection area to northwestern Mexico and southwestern U.S., when the Mexican (or North American) monsoon season is well established (Cortez, 2000, and references within). This northward displacement of the high-pressure causes easterly winds over the NETP region between ~11°N and 18°N and north-easterlies over the Gulf of Mexico during these months. The September 200-mb surface map resembles that of June, with some differences in the Gulf of Mexico and western Caribbean where less intense winds are observed.

The geopotential height anomalies from the June-September mean as a function of height (Fig. 8), display an interesting spatial pattern. While the upper level anomalies present a fairly zonal distribution, at low levels the patterns appear to be influenced by the land/ocean distribution (as seen in Fig. 6), with topographic influence evident even in the 700-mb maps. The months of July and August show a complete reversal in the sign of the anomalies compared with June at all levels.
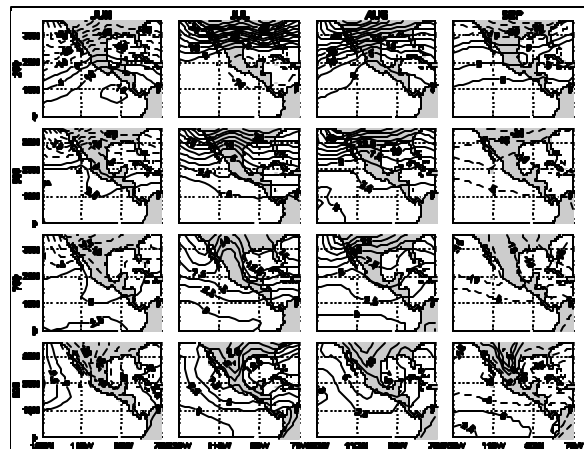

Figure 8. Geopotential height anomalies with regard to the Jun-Sep mean for June through September for the 925, 700, 500, and 200-mb surfaces from ERA-40 data.

The anomalies during mid-summer are positive north of 10°-15°N throughout the troposphere and display a slight tilt with height towards the north, with maximum anomalies at 500-mb and upper levels located north of 35°N. In September the anomalies revert back to negative throughout the troposphere (north of

10°N), again indicating a strong zonal component and the axis of minimum anomaly tilting towards the north at higher levels. The changes in the sign of the anomalies appear very sudden, with sharp transitions from one phase between June and July and back to a similar June phase between August and September. There is no evidence of propagation in the anomalies, since all levels present the same sign of the anomalies simultaneously. These patterns suggest that the regional, mid-summer, low-level wind patterns observed in the NETP are likely the result of large scale perturbations present within the whole domain of the study and throughout the troposphere and are not dominated by local forcings.

4. SUMMARY

The unprecedented high quality and space-time resolution of the QSCAT winds allow the study of large and small-scale atmospheric dynamical processes, with a significant precision, over otherwise poorly sampled oceanic regions. In this study, QSCAT data from August 1999 through December 2004 are used to analyze the mean characteristics of the wind jets off the Pacific coasts of southern Mexico and Central America and the low-level circulation over the NETP during summer, making a comparison with their winter features.

Climatological vector winds and divergence show that, during boreal winter, the wind jets over the Gulfs of Tehuantepec, Papagayo, and Panama significantly influence the position and shape of the ITCZ in the far NETP. In particular, the Tehuantepec and Papagayo jets keep the ITCZ confined to the south of the jets, and the Panama jet forms a divergence patch over the January-April ITCZ. It is observed that the Tehuantepec jet merges with the Papagayo jet and both become integrated to the northerly trades flow. During winter and spring months (December-April), when the northeast trades are strong and reach their maximum southward penetration, winds over the NETP are mainly directed toward the western Pacific moving away from the coasts. From April, the ITCZ begins to migrate northward and the southerly trades to intensify. In June, when southerly trades are relatively intense and northerly trades are relatively weak, a slight wind direction reversal over the NETP is observed, around 10°N and east of ~116°W (Fig. 2f), favoring the

moisture transport toward the continent and coinciding with the onset of the rainfall season in central-southern Mexico and Central America.

Although the jets become weaker toward the summer, climatological winds show a slight intensification over the gulfs of Tehuantepec and Papagayo during July-August. The wind and divergence fields suggest that the mid-summer strengthening of the jets induces a slight easterly low-level circulation over the NETP, which, extending from the continent to around 113°W between 10°N and 15°N, inhibits the low-level moisture transport to the continent and seems to block the northward penetration of the southeast trades, despite their considerable strength. This change in the circulation pattern coincides with, and partially explains, the mid-summer drought observed in southern Mexico and Central America during late July-early August.

Long-term monthly mean SLP and SLP anomaly maps from ERA-40, show that the mid-summer intensification of the Tehuantepec and Papagayo jets is due to the maximum westward extension and strengthening of the Azores-Bermuda high (ABH) over the subtropical Atlantic during this time of the year. In July, a SLP positive anomaly reaching the far-eastern NETP and increasing toward the northeastern Atlantic produces a pressure gradient across the Isthmus of Tehuantepec that induces the strengthening of the Tehuantepec jet. However, there is no such across-gap pressure gradient that might induce the mid-summer intensification of the Papagayo jet, suggesting that this jet is generated by a different mechanism, as was previously proposed by Chelton, et al. (2000a). Due to the meridional orientation of the Tehuantepec gap, the across-gap pressure gradient induces a northerly jet that flows perpendicular to the isobars, while the zonally oriented Papagayo gap favors the funneling of the western Caribbean zonal winds flowing roughly parallel to the ABH isobars.

Geopotential height and wind data for different upper atmospheric levels from the ERA-40, show that pressure and wind anomalies are observed at all levels during the mid-summer months. The cause of the observed three-dimensional structure of the geopotential anomalies and the sudden change in phase in the mid-summer months are not completely

understood yet. Further study will involve the impact that the anomalies associated with large-scale features, such as the Northern Hemisphere annular mode, would exert on the particular region of the Gulf of Mexico-Caribbean Sea and the NETP.

To conclude, data show that the mid-summer intensification of the Tehuantepec and Papagayo gap winds is the result of changes in the large-scale atmospheric circulation, characterized by a pressure anomaly over the subtropical Atlantic that extends westward reaching the far-eastern tropical Pacific. The easterly low-level circulation pattern induced by this anomaly over the NETP has important implications regarding moisture transports. Identifying large-scale influences could lead to improvement in the understanding of implications for the interannual, seasonal and intraseasonal variability of other variables, such as precipitation in the region.

REFERENCES

Amador, J. A., E. J. Alfaro, O. G. Lizano, and V. O. Magaña, 2005: Atmospheric forcing of the eastern tropical Pacific: A review, *Progress in Oceanography*, Special Issue: Review of Eastern Tropical Pacific Oceanography. P. Fiedler and M. Lavín Eds., Pergamon, in press.

Bourassa, M. A., D. M. Legler, J. J. O'Brien, and S. R. Smith, 2003: SeaWinds Validation with research vessels. *J. Geophys. Res.*, **108**(C2), 3019, doi:10.1029/2001JC001028.

Chelton, D. B., M. H. Freilich, and S. K. Esbensen, 2000a: Satellite observations of the wind jets off the Pacific coast of Central America. Part I: Case studies and statistical characteristics. *Mon. Wea. Rev.*, **128**, 1993–2018.

—, —, and —, 2000b: Satellite observations of the wind jets off the Pacific coast of Central America. Part II: Regional relationships and dynamical considerations. *Mon. Wea. Rev.*, **128**, 2019–2043.

Chelton, D. B., M. G. Schlax, M. H. Freilich, and R. F. Milliff, 2004: Satellite measurements reveal persistent small-scale features in ocean winds, *Science*, **303**, 978-983.

Clarke, A. J., 1988: Inertial wind path and sea surface temperature patterns near the Gulf of Tehuantepec and Gulf of Papagayo. *J. Geophys. Res.*, **93**, 15 491–15 501.

Cortez, M., 2000: Variaciones intraestacionales de la actividad convectiva en México y América Central. *Atmósfera*, **13**(2), 95-108.

Curtis, S., 2004: Diurnal cycle of rainfall and surface winds and the mid-summer drought of Mexico/Central America. *Clim. Res.*, **27**, 1-8.

Kessler, W. S., 2002: Mean three-dimensional circulation in the northeast tropical Pacific, *J. Phys. Oceanogr.*, **32**, 2457-2471.

Lavín, M. F., and Coauthors, 1992: Física del Golfo de Tehuantepec. *Cienc. Desarrollo*, **17**, 97–108.

Magaña, V., J. Amador, and S. Medina, 1999: The midsummer drought over Mexico and Central America. *J. Climate*, 12, 1577–1588.

Magaña, V. and E. Caetano, 2005: Temporal evolution of summer convective activity over the Americas warm pools. *Geophys. Res. Lett.*, **32**, L02803, doi:10.1029/2004GL021033.

Parmenter, F. C., 1970: Picture of the month: A "Tehuantepecer". *Mon. Wea. Rev.*, **98**, 479.

Roden, G. I., 1961: On the wind driven circulation in the Gulf of Tehuantepec and its effect upon surface temperatures. *Geofis. Int.*, **1**(3), 55–76.

Romero-Centeno, R., J. Zavala-Hidalgo, A. Gallegos, and J. J. O'Brien, 2003: Isthmus of Tehuantepec wind climatology and ENSO signal. *J. Climate*, **16**, 2628-2639.

Schultz, D. M., W. E. Bracken, L. F. Bosart, G. J. Hakim, M. A. Bedrick, M. J. Dickinson, and K. R. Tyle, 1997: The 1993 superstorm cold surge: Frontal structure, gap flow, and tropical impact. *Mon. Wea. Rev.*, **125**, 5–39; Corrigendum, 125, 662.

Steenburgh, W. J., D. M. Schultz, and B. A. Colle, 1998: The structure and evolution of gap outflow over the Gulf of Tehuantepec, Mexico. *Mon. Wea. Rev.*, **126**, 2673–2691.

Xie, S-P., H. Xu, W. S. Kessler, and M. Nonaka, 2005: Air-sea interaction over the eastern Pacific warm pool: Gap winds, thermocline dome, and atmospheric convection. *J. Climate*, **18**(1), 5-20.